

Communication

Rechargeable solid-state lithium metal batteries with vertically aligned ceramic nanoparticle/polymer composite electrolyte



Xue Wang^{a,b}, Haowei Zhai^a, Boyu Qie^a, Qian Cheng^a, Aijun Li^a, James Borovilas^a, Bingqing Xu^a, Changmin Shi^a, Tianwei Jin^a, Xiangbiao Liao^a, Yibin Li^b, Xiaodong He^b, Shanyi Du^b, Yanke Fu^a, Martin Dontigny^c, Karim Zaghib^c, Yuan Yang^{a,*}

^a Department of Applied Physics and Applied Mathematics, Columbia University, New York, NY, 10025, USA

^b School of Astronautics, Harbin Institute of Technology, Harbin, 150001, PR China

^c IREQ—Institute Recherche d'Hydro-Québec, Varennes, Québec, J3X 1S1, Canada

ARTICLE INFO

Keywords:

Ice-templating
Composite electrolytes
Solid state batteries
Energy storage

ABSTRACT

Composite solid electrolytes are attractive as they combine the high ionic conductivity of ceramic nanoparticles and the excellent mechanical properties of polymer electrolytes. Vertically aligned ceramic nanoparticles in the polymer matrix represent an ideal structure for maximizing ionic conductivity of composite electrolytes. The ice-templating method was used to build rechargeable solid-state lithium metal batteries with a vertically aligned ceramic/polymer composite electrolyte composed of high ionic conductivity $\text{Li}_{1.5}\text{Al}_{0.5}\text{Ge}_{1.5}(\text{PO}_4)_3$ (LAGP) and polyethylene oxide (PEO) polymer. The vertical LAGP walls provide continuous channels for fast ionic transport, while the PEO matrix renders the composite electrolyte flexible. This solid-state composite electrolyte has a conductivity of $1.67 \times 10^{-4} \text{ S cm}^{-1}$ at room temperature and $1.11 \times 10^{-3} \text{ S cm}^{-1}$ at 60°C . LiFePO_4 (LFP)/vertically aligned LAGP-PEO/Li full cells were also developed with a high capacity retention of 93.3% after 300 cycles. This study demonstrates the successful application of vertically aligned ceramic/polymer composite electrolytes for solid-state batteries with high performance.

1. Introduction

Lithium-based rechargeable batteries with high energy density play an important role in many applications including electric vehicles, grid-level energy storage, and communications [1]. Among various electrode materials lithium metal anode is highly attractive as it offers ten times the specific capacity (3860 mAh g^{-1}) as that of the state-of-the-art graphite anode (372 mAh g^{-1}) [2,3], however, lithium metal tends to form dendrites during the charging process. Flammable organic liquid electrolytes in Li-ion batteries fail to suppress dendrite formation, leading batteries to short, causing fires and explosions [4–6]. To address this challenge, thermally stable solid state electrolytes (SSEs) are an attractive solution [7,8]. SSEs are also mechanically stronger, enabling them to suppress dendrite formation and significantly extend the cycling stability and lifetime of rechargeable lithium batteries [9].

Increased interest in solid electrolytes has led to development of ceramic electrolytes such as sulfides [10,11], perovskite $\text{Li}_{3-x}\text{La}_{2/3-x}\text{TiO}_3$ [12], garnet-type $\text{Li}_5\text{La}_3\text{Zr}_2\text{O}_{12}$ [13,14], $\text{Li}_{1+x}\text{Al}_x\text{Ti}_{2-x}(\text{PO}_4)_3$, and $\text{Li}_{1+x}\text{Al}_x\text{Ge}_{2-x}(\text{PO}_4)_3$ [15–17] with high ionic conductivity of 10^{-4} –

$10^{-2} \text{ S cm}^{-1}$ [18,19]. Their mechanical properties and interfacial impedance with electrodes, however, are undesirable [20,21]. As a result, large-scale manufacturing remains a challenge. In contrast to ceramic electrolytes, polymer electrolytes, which combine polymers (e.g. polyester, polyether) with lithium salts (e.g. LiClO_4 , LiAsF_6 , and LiPF_6) [22], are light, elastic, and compatible with state-of-the-art manufacturing processes [23]. Their ionic conductivities, however, are typically low, on the order of 10^{-6} – $10^{-5} \text{ S cm}^{-1}$ at room temperature [24–26].

Various strategies have been studied to fabricate polymer/ceramic composite electrolytes to leverage the advantages of these two types of solid electrolytes, including the electrospun ceramic electrolyte nanowires/polymer composition and the addition of ceramic electrolyte nanoparticles into a polymer matrix [27–32]. Chen Zi Zhao et al. proposed a flexible anion-immobilized ceramic–polymer composite electrolyte with excellent specific capacities to inhibit lithium dendrites and construct safe batteries [33]. Jiwoong Bae et al. designed a three-dimensional nanostructured garnet framework composite polymer electrolyte with an improved conductivity of $8.5 \times 10^{-5} \text{ S cm}^{-1}$ at 25°C

* Corresponding author.

E-mail address: yy2664@columbia.edu (Y. Yang).

<https://doi.org/10.1016/j.nanoen.2019.03.051>

Received 18 December 2018; Received in revised form 5 March 2019; Accepted 13 March 2019

Available online 18 March 2019

2211-2855/© 2019 Published by Elsevier Ltd.

[34]. Analysis of tortuosity suggests vertically aligned and interconnected ceramic particles are the optimal configuration to create pathways of high ionic conductivity, while the polymer phase provides mechanical support and flexibility. This is supported by recent studies on the ionic conductivity of a LLTO nanofiber/PEO electrolyte, in which aligned LLTO fibers increased ionic conductivity from $1.78 \times 10^{-7} \text{ S cm}^{-1}$ to $6.05 \times 10^{-5} \text{ S cm}^{-1}$ at 30° C [35]. Xiaokun Zhang et al. filled an anodic aluminum oxides template with PEO electrolyte and showed that the vertical interfaces with high conductivity enhanced ionic conductivity of the whole composite by one order of magnitude [36]. The present study demonstrates vertically aligned LAGP nanoparticles imbedded in a PEO matrix with a ionic conductivity of $1.67 \times 10^{-4} \text{ S cm}^{-1}$ at room temperature. The composite electrolyte was then combined with a lithium anode and a LiFePO_4 cathode to form a full cell, which successfully ran for 300 cycles with only 6.7% loss in capacity.

2. Experimental description

2.1. Materials and chemicals

Poly(ethylene glycol) (PEG, Mw 400), Poly(ethylene glycol) dimethyl ether (PEGDME, Mw 500), Poly(ethylene oxide) (PEO, Mw 600,000), acetonitrile (anhydrous, 99.8%), Poly(vinyl alcohol) (PVA, Mw, 85,000–124,000), 1-Octanol, Lithium bis(trifluoromethanesulfonyl)imide (LiTFSI), 2,4,7,9-tetramethyl-5-decyne-4,7-diol ethoxylate were received from Sigma-Aldrich. LAGP (200–500 nm) were purchased from MTI corporation. LiFePO_4 particles were provided by Hydro-Québec.

2.2. Electrolyte preparation

The starting suspension of ice templated PEO/LAGP electrolyte was composed of 3.5 wt % PVA as binder, 60 wt % H_2O , 2.5 wt % PEG (Mw, 400) as plasticizer, 4.9 wt % 2,4,7,9-tetramethyl-5-decyne-4,7-diol ethoxylate as surface active agent, and 1 wt % 1-Octanol as defoaming agent. LAGP (26 wt %) was then added into the starting suspension and stirred to achieve homogeneity. Using a doctor-blade, the suspension was coated onto an Al_2O_3 substrate, which was then placed on the thermoelectric plate of an ice-templating device at a cooling rate of 3° C/min . After the suspension stayed at -20° C for 10 min, ice crystals were removed by vacuum drying; the resulting porous LAGP film was sintered at 800° C for 5 h. The polymer solution of PEO (Mw = 600,000)/PEGDME (Mw ~ 500)/LiTFSI in acetonitrile was added on the upper and lower surfaces of the LAGP sample. The weight ratio of PEO : PEG = 1:1, and the molar ratio of ethylene oxide (EO) to LiTFSI = 8:1. The electrolyte samples were dried in a desiccator for 12 h. To remove trace amount of residual water, the electrolyte was further heated at 80° C for 24 h and allowed to rest for another 48 h inside a glovebox before testing.

For the random PEO/LAGP electrolyte, 0.16 g PEO (Mw, 600,000) and 0.16 g PEGDME-500 were dissolved in acetonitrile and stirred at 50° C for 6 h. 0.13 g LiTFSI and 0.68 g LAGP were then added into the PEO/PEG acetonitrile solution and stirred for another 4 h. The prepared suspension was casted into a Teflon mold, and dried in a desiccator for 12 h. The process of removing acetonitrile and water was the same as above.

2.3. Material characterization

SEM images were acquired by a Zeiss SIGMA VP scanning electron microscope, with EHT at 3 kV during the measurement. The TGA measurement was carried out by a TA Instrument Q500. All samples were tested under O_2 atmosphere with a heating rate of 10° C/min . The crystal structures of the synthesized materials were characterized by PANalytical XPert 3 Powder XRD.

2.4. Battery fabrication

Symmetric stainless steel/electrolyte/stainless steel cells were assembled for EIS measurements in the pouch cell configuration. Cyclic voltammetry measurements were performed in lithium/SPE/stainless steel cells in the coin cell configuration. The lithium metal anode used in half-cell cycling was $250 \mu\text{m}$ in thickness and the LiFePO_4 (LFP) cathode was 2.53 mg cm^{-2} ($\sim 0.4 \text{ mAh cm}^{-2}$). LFP cathode was assembled by slurring the active material (80 wt% LFP, 10 wt% carbon black, and 10 wt% Polyvinylidene fluoride (PVDF)) in *N*-methyl-2-pyrrolidone (NMP) and coating onto the aluminum substrate. The NMP was evaporated at 110° C and then the electrode was punched with a diameter of 12 mm. To achieve a good contact between LFP and electrolyte, molten PEO/LiTFSI (EO/Li = 8:1, PEO Mw = 10,000) at 150° C was quickly added onto the cathode surface prior to cell assembly. The electrode was then heated at 110° C for 4 h to let the molten solution penetrate into pores in the LFP electrode. All procedures were carried out in an argon-filled glovebox with $\text{O}_2 < 0.1 \text{ ppm}$ and $\text{H}_2\text{O} < 0.1 \text{ ppm}$.

2.5. Electrochemical characterizations

The EIS and cyclic voltammetry were measured by a Bio-logic VMP3 potentiostat at voltage amplitude of 10 mV and a frequency range of 1 MHz – 0.1 Hz. The cyclic voltammetry was measured between -0.2 V and 4.5 V vs. Li/Li^+ at 60° C with a scan rate of 5 mV/s. Galvanostatic cycling was conducted on a standard eight-channel LAND battery testing system (CT2001A). The voltage range was 2.5–3.8 V at 60° C . The cell temperature was controlled by a gravity convection oven (DHG-9015, MTI Corporation).

3. Results and discussion

Fig. 1 illustrates the process of preparing the ice-templated ceramic nanoparticles/polymer composite electrolyte. The ice-templating process has been used to form vertical structures for battery electrodes and other functional materials in previous studies [37–40]. The starting suspension of ice templated PEO/LAGP electrolyte was coated onto an Al_2O_3 substrate, and cooled at a preset speed controlled by a thermoelectric plate (Fig. S1). Freezing the suspension caused ice crystals to grow from the bottom and eject the LAGP nanoparticles to the side, forming vertical walls. The ice was then removed by vacuum drying, and a porous structure with vertically aligned LAGP was obtained. The porous film was further annealed at 800° C for 5 h to densify the film and form better connections among LAGP nanoparticles, which facilitated the transport of lithium ions. Finally, PEO-based polymer electrolyte was drop cast onto the porous film to fill into all pores to provide mechanical support and reduce interfacial resistance among LAGP particles. To form a good contact at the lithium/electrolyte interface, 10–20% more PEO-based polymer solution was added in the PEO/LAGP electrolyte.

The samples at different stages were first characterized by a scanning electron microscope (SEM) to verify the vertical alignment of the structure. Fig. 1b and c indicate that well-defined vertically aligned LAGP walls spaced 10–20 μm from each other are formed after ice templating. After annealing at 800° C , the binder and the plasticizer were removed and LAGP nanoparticles were better sintered together. The vertically aligned structure can still be observed in top view and cross-sectional view (Fig. 1d and e). Then LiTFSI/PEO/PEG polymer is filled inside by drop casting (Fig. 1f and g), where the weight ratio of PEO: PEG is 1:1, and the molar ratio of ethylene oxide and LiTFSI is 8:1. As a result, a composite solid electrolyte with vertically aligned ceramic electrolyte filler is successfully prepared. Thermogravimetric analysis (Fig. S2) shows that the resulting samples contain a 40 vol% of LAGP nanoparticles. The volumetric percentage can vary from 10 to 60% by changing the proportion of ceramic nanoparticles and water, the rate of

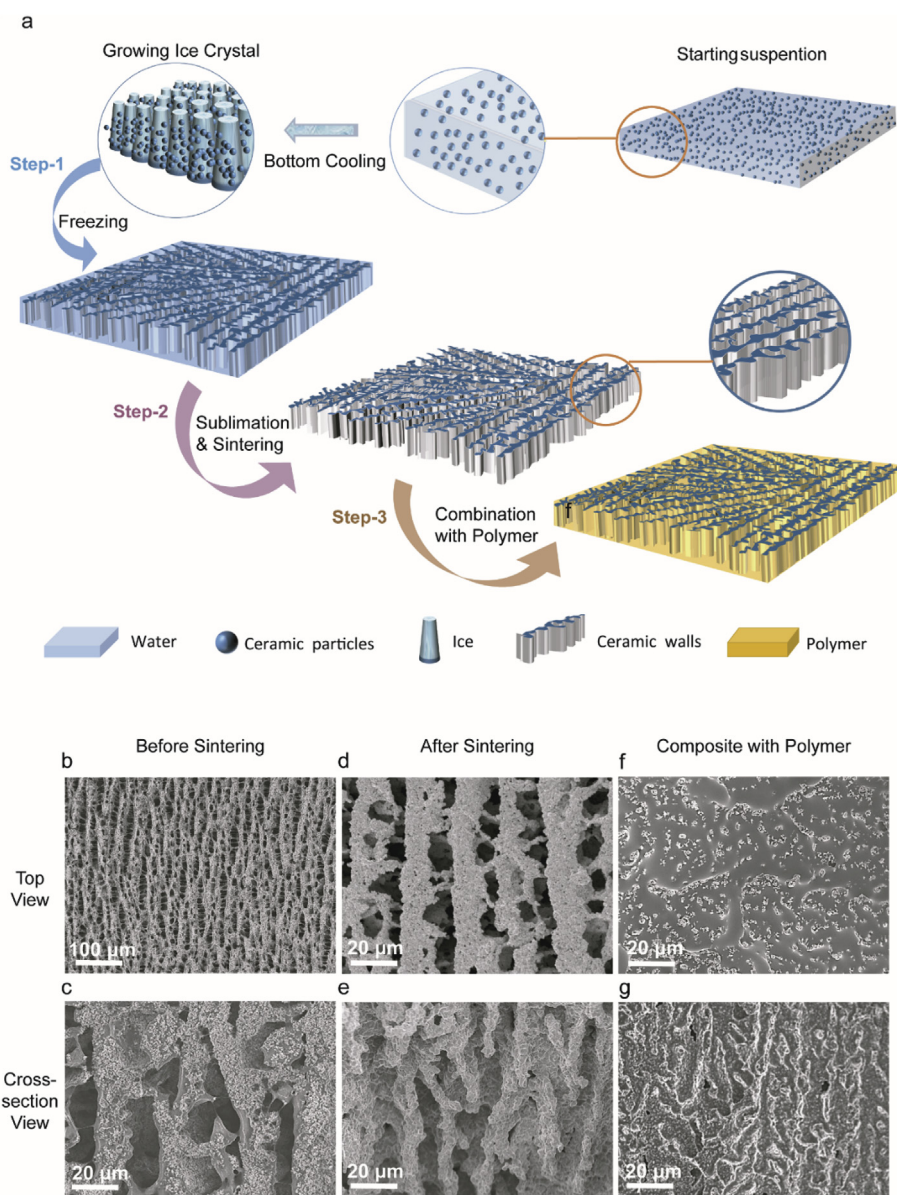


Fig. 1. The fabrication and characterization of ice-templated ceramic/polymer composite electrolyte. (a) The schematic of preparation process of the ice-templated LAGP/PEO composite electrolyte. (b) Top view and (c) cross-sectional view of ice templated LAGP before sintering. (d) Top view and (e) cross-sectional view of ice templated LAGP nanoparticles after sintering. (f) Top view and (g) cross-section view of the solid electrolyte after combining with PEO/PEG/LiTFSI.

cooling during the ice-templating process and the sintering temperature, which have been studied in the past [41–45], demonstrating the flexibility of using ice templating to achieve desired compositions.

The electrochemical impedance spectroscopy (EIS) of stainless steel/ice-templated LAGP/PEO composite electrolyte film/stainless steel cells was measured at different temperatures to determine that the vertically aligned structure could facilitate the transport of Li^+ ions and enhance the electrolyte's ionic conductivity. The typical sample size was 1 cm^2 and the thickness was between 100 and $200 \mu\text{m}$. The room temperature conductivity reaches $1.67 \times 10^{-4} \text{ S cm}^{-1}$ at 120Ω in Fig. 2a. As the sintered LAGP pellet and the PEO-based polymer electrolyte have ionic conductivities of $3.37 \times 10^{-4} \text{ S cm}^{-1}$ (Fig. S3) and $1.92 \times 10^{-5} \text{ S cm}^{-1}$ (Fig. S4), respectively, and LAGP occupies 40% in volume, therefore, the theoretical conductivity of a perfectly vertically aligned LAGP phase is $1.46 \times 10^{-4} \text{ S cm}^{-1}$. This theoretical value is consistent with the experimental value of the ice-templated LAGP/PEO composite electrolyte.

The temperature-dependent EIS measurements shows that the ionic conductivity of ice templated LAGP/PEO reaches $1.11 \times 10^{-3} \text{ S cm}^{-1}$ at 60°C . The corresponding activation energy (E_a) is 0.45 eV based on the Arrhenius plots in Fig. 2c, while the activation energy of pure LAGP, PEO/PEG/LiTFSI polymer, and PEO with randomly distributed LAGP are 0.32 eV, 0.99 eV and 0.68 eV, respectively (Fig. 2c, Fig. S3). As E_a of vertically aligned LAGP/PEO is closer to pure LAGP, this indicates that Li^+ ions mainly move through the LAGP phase.

The conductivity of ice-templated LAGP film soaked in a dilute organic liquid electrolyte ($2.47 \times 10^{-6} \text{ S cm}^{-1}$), as the film itself is too fragile to conduct measurements of intrinsic conductivity prior to combining with polymer, was measured to determine whether LAGP contributes most to ionic conduction. The measurements yielded a conductivity of $1.22 \times 10^{-4} \text{ S cm}^{-1}$ (Fig. S5). Based on the porosity (60%) of the film, the corresponding conductivity of the LAGP bulk phase is estimated to be $2.9 \times 10^{-4} \text{ S cm}^{-1}$, which is consistent with previous conductivity measurements of the LAGP pellet (Fig. S1). This

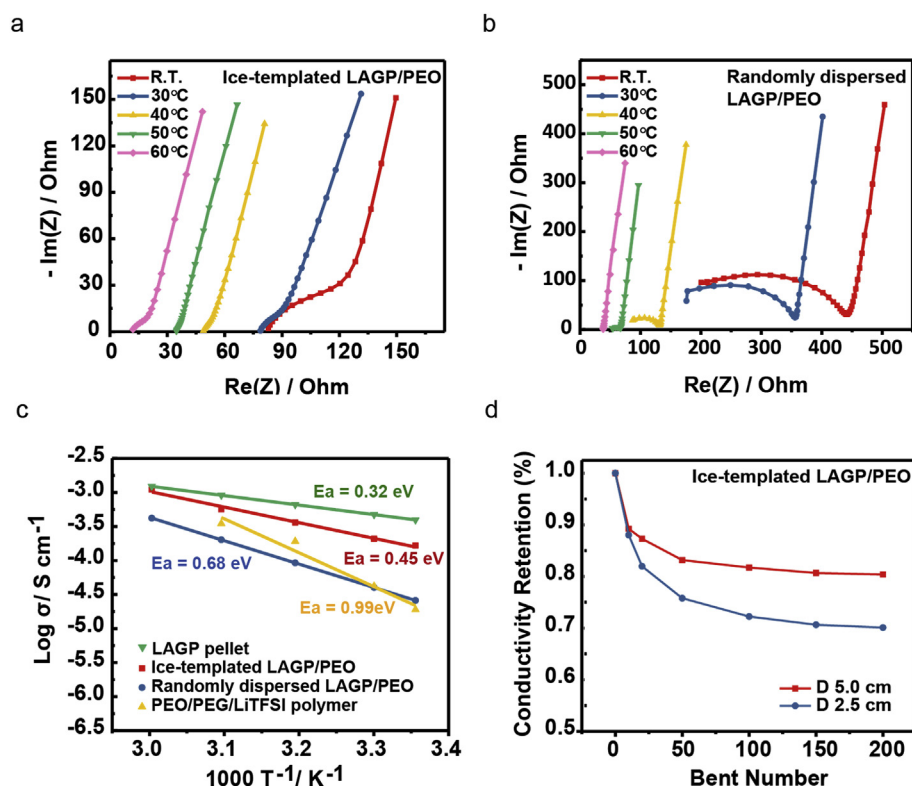


Fig. 2. (a) EIS of a SS/ice-templated LAGP/PEO composite electrolytes/SS cell at different temperatures. The frequency range is 1 MHz - 0.1 Hz. (b) EIS of a stainless steel (SS)/randomly dispersed composite electrolytes/SS cell at different temperatures. The frequency range is 1 MHz - 0.1 Hz. (c) Arrhenius plots of the ice-templated LAGP/PEO, randomly dispersed LAGP/PEO and polymer electrolytes. (d) Ionic conductivity after bending for different times.

indicates that the high conductivity of the ice-templated composite can be attributed primarily to LAGP phase.

Continuous pathway in vertically aligned LAGP nanoparticles lead to higher ionic conductivity compared to other configurations, such as random LAGP/PEO (conductivity = $2.7 \times 10^{-5} \text{ S cm}^{-1}$ at room temperature (Fig. 2b, Fig. S6)), as the ion conduction is mainly impeded by the polymer phase with low ionic conductivity. Compared to random distribution LAGP/PEO, the interconnected particles in the vertically aligned structure result in a conductivity increase of nearly 620%.

The conductivity of the ice-templated LAGP/PEO is similar with the previous work on vertically aligned anodized aluminum oxide (AAO)/polymer composite electrolyte, which has an ionic conductivity of $1.79 \times 10^{-4} \text{ S cm}^{-1}$ at room temperature [36]. Meanwhile, it is 2.8 times higher than the polymer electrolytes with well-aligned ceramic nanowires, 30 times higher as that with randomly ceramic nanowires [35]. The ice-templated composite electrolyte also behaves better when compared with randomly ceramic-particles/polymer electrolytes, such as LLZTO/PEO and LLZO/PEO [46–48]. However, as the plasticizer used are difference, the comparisons should be just used as references.

In addition to the relatively high ionic conductivity, ice-templated LAGP/PEO composite solid electrolyte also has a Li-ion transference number (t_+) of 0.56, while the randomly dispersed LAGP/PEO electrolyte has a lithium-ion transference numbers of 0.33 (Fig. S7 and Table S1). This is better than previous work on polyacrylonitrile (PAN) polymer electrolytes with well-aligned $\text{Li}_{0.33}\text{La}_{0.557}\text{TiO}_3$ (LLTO) ceramic nanowires ($t_+ = 0.42$) and PAN polymer electrolytes with random LLZO ceramic nanowires ($t_+ = 0.42$) [35,49]. Therefore, the vertically aligned structure also improves the portion of lithium ions in the ion conduction.

The electrochemical stability of the LAGP/PEO composite electrolyte was further characterized by cyclic voltammetry at 60 °C. Lithium metal foil and stainless steel were used as the counter electrode and the working electrode, respectively. As shown in Fig. S8, the peak between -0.2 V and 1 V vs. Li^+/Li is attributed to lithium deposition and dissolution. In addition, no redox peak or obvious side reaction is observed between 1 and 4.5 V vs Li^+/Li . These results confirm that the composite

electrolyte is stable up to 4.5 V vs. Li^+/Li and can be combined with conventional cathode materials in lithium ion batteries.

The membrane also shows reasonable flexibility, determined through measurements of ionic conductivity after bending to a specific diameter a certain number times (Fig. 2d). When bent down to a diameter of 5 cm for 50 times and 200 times, the resulting conductivities remain at 83.2% and 80.4% respectively of the conductivity measured before bending. Similar behavior is also observed when the sample was bent down to a diameter of 2.5 cm . The conductivity is reduced to 75.8% after 50 cycles, but remains at 70.1% after 200 cycles. This suggests the initial bending leads to small cracks of ceramic phase inside the composite electrolyte, which can readily release stress inside. Once the cracks of ceramic phase are stabilized, the conductivity reaches a steady state without further deterioration.

To demonstrate real applications in batteries, the electrochemical performance of the ice-templated LAGP/PEO electrolyte was first tested in the lithium/lithium cell at 60 °C. As shown in Fig. 3a, the Li - LAGP/PEO - Li symmetric cell has a steady performance under long term of cycling. At a current density of 0.1 mA cm^{-2} and 2-h cycling, the average cell voltage maintains at 0.17 V for 200 h without any increase. When the current density and deposited capacity further increase to 0.3 mA cm^{-2} and 0.3 mAh cm^{-2} , respectively, the average overpotential is steady at 0.39 V for another 200 h. The steady performance in symmetric Li - Li cells supports the results of cyclic voltammetry, showing that the prepared PEO/LAGP electrolyte can be cycled for long time with lithium metal anode.

The LAGP/PEO composite electrolyte is further combined with lithium metal anode and LiFePO_4 cathode to assemble full solid-state cells. In the cycling test the cell has an initial specific capacity of 148.7 mAh g^{-1} at 0.2 C for the first cycle. As the current increases to 0.3 C , the initial specific capacity is 148.7 mAh g^{-1} and remains at 138.8 mAh g^{-1} after 300 cycles, corresponding to a capacity retention of 93.3% (Fig. 3b). These results verify that the synthesized composite electrolyte could successfully bear high voltage and long cycling, not only with lithium metal but also with LFP cathode. The voltage hysteresis also remains steady at $\sim 0.15 \text{ V}$ from the 1st cycle to the 300th cycle

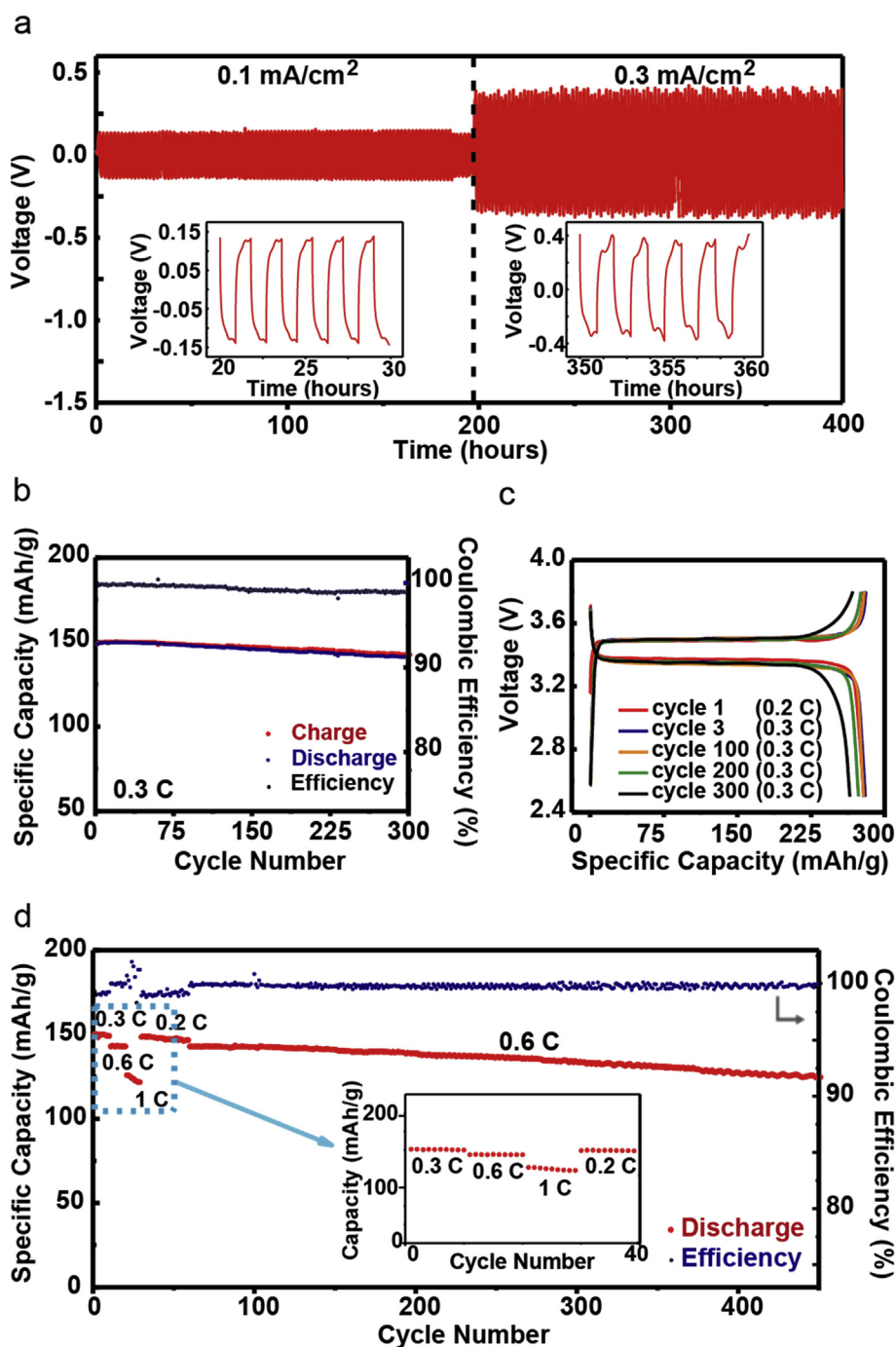


Fig. 3. Electrochemical characterizations of the LAGP/PEO composite electrolyte in Li/Li symmetric cells and Li/LiFePO₄ cells at 60 °C. (a) Voltage profiles and the zoom-in profile of a Li-LAGP/PEO-Li cell at current densities of 0.1 and 0.3 mA/cm², respectively. Each cycle includes 1-h charging and 1-h discharging. (b) The cycling performance of Li-LAGP/PEO-LiFePO₄ full-cell between 2.5 V to 3.8 V vs Li⁺/Li. (c) Galvanostatic charge and discharge profiles of Li-LAGP/PEO-LiFePO₄ at 0.2 C for the first 2 cycles and 0.3 C for the following 300 cycles between 2.5 V to 3.8 V vs Li⁺/Li. (d) The rate capacity of a Li-LAGP/PEO-LiFePO₄ full-cell cycled at 0.3, 0.6 and 1 C, followed by 400 cycles at 0.6 C.

(Fig. 3c). The steady capacity and voltage hysteresis demonstrate the robustness of the PEO/LAGP composite electrolyte for long term operation in lithium batteries. Rate performance further shows the composite electrolyte can function well up to at least 1 C. The specific capacities reach 150.6 mAh g⁻¹, 139.0 mAh g⁻¹ and 123.7 mAh g⁻¹ at rates of 0.3 C, 0.5 C, and 1 C, respectively (Fig. 3d). The same cell subsequently shows steady performance for more than 400 cycles at 0.6 C. The capacity is seen to decrease at a rate of only 3.2% per 100 cycles. Further tests with higher mass loading (e.g. 0.9 mAh cm⁻²) show that the overpotential is higher (Fig. S10) and thus that more optimization (e.g. thinner electrolyte) is needed to achieve high performance with high mass loading (e.g. 2 mAh cm⁻², 2 mA cm⁻²). In addition, further tests with lithium anode whose capacity is close to that of the cathode are needed to evaluate performance in practical

cells.

4. Conclusions

In summary, this paper presents the study of rechargeable solid-state batteries with vertically aligned ceramic/polymer composite electrolyte, composed of ice-templated LAGP vertically aligned walls and flexible PEO/PEG polymer. The aligned ceramic phase in the composite electrolyte allows fast conduction of lithium ions. The conductivity reaches 1.67×10^{-4} S cm⁻¹ at room temperature, 6.9 times of that with LAGP randomly dispersed inside. The vertically aligned LAGP nanoparticles/PEO cell shows a steady performance in both Li-Li symmetric cell and Li/LiFePO₄ cells. The capacity retention reaches 87.4% after 400 cycles at 0.6 C in full cells. These results demonstrate

that ice templating is a viable approach in fabricating composite electrolyte with high ionic conductivity for solid state rechargeable lithium batteries.

Acknowledgements

Y. Yang acknowledges the funding support from AFOSR (FA9550-18-1-0410). Xue Wang thanks the financial support from China Scholarship Council during her study (CSC, No. 201706120088).

Appendix A. Supplementary data

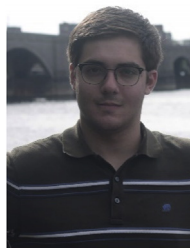
Supplementary data to this article can be found online at <https://doi.org/10.1016/j.nanoen.2019.03.051>.

References

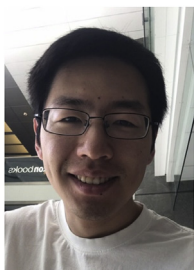
- [1] K. Liu, Y. Liu, D. Lin, A. Pei, Y. Cui, Materials for lithium-ion battery safety, *Science Advances* 4 (2018) eaas9820.
- [2] M. Armand, J.-M. Tarascon, Building better batteries, *Nature* 451 (2008) 652.
- [3] F. Han, J. Yue, C. Chen, N. Zhao, X. Fan, Z. Ma, T. Gao, F. Wang, X. Guo, C. Wang, Interphase engineering enabled all-ceramic lithium battery, *Joule* 2 (2018) 497–508.
- [4] C. Yuqin, L. Hong, W. Lie, L. Tianhong, Irreversible capacity loss of graphite electrode in lithium-ion batteries, *J. Power Sources* 68 (1997) 187–190.
- [5] E.J. Berg, C. Villeveille, D. Streich, S. Trabesinger, P. Novák, Rechargeable batteries: grasping for the limits of chemistry, *J. Electrochem. Soc.* 162 (2015) A2468–A2475.
- [6] F. Luo, B. Liu, J. Zheng, G. Chu, K. Zhong, H. Li, X. Huang, L. Chen, Nano-silicon/carbon composite anode materials towards practical application for next generation lithium batteries, *J. Electrochem. Soc.* 162 (2015) A2509–A2528.
- [7] H. Wu, G. Chan, J.W. Choi, I. Ryu, Y. Yao, M.T. McDowell, S.W. Lee, A. Jackson, Y. Yang, L. Hu, Stable cycling of double-walled silicon nanotube battery anodes through solid–electrolyte interphase control, *Nat. Nanotechnol.* 7 (2012) 310.
- [8] Y. Sun, Lithium ion conducting membranes for lithium-air batteries, *Nanomater. Energy* 2 (2013) 801–816.
- [9] J.G. Kim, B. Son, S. Mukherjee, N. Schuppert, A. Bates, O. Kwon, M.J. Choi, H.Y. Chung, S. Park, A review of lithium and non-lithium based solid state batteries, *J. Power Sources* 282 (2015) 299–322.
- [10] J.W. Fergus, Ceramic and polymeric solid electrolytes for lithium-ion batteries, *J. Power Sources* 195 (2010) 4554–4569.
- [11] L. Suo, Y.-S. Hu, H. Li, M. Armand, L. Chen, A new class of solvent-in-salt electrolyte for high-energy rechargeable metallic lithium batteries, *Nat. Commun.* 4 (2013) 1481.
- [12] W. Liu, N. Liu, J. Sun, P.-C. Hsu, Y. Li, H.-W. Lee, Y. Cui, Ionic conductivity enhancement of polymer electrolytes with ceramic nanowire fillers, *Nano Lett.* 15 (2015) 2740–2745.
- [13] S. Ohta, T. Kobayashi, J. Seki, T. Asaoka, Electrochemical performance of an all-solid-state lithium ion battery with garnet-type oxide electrolyte, *J. Power Sources* 202 (2012) 332–335.
- [14] I. Kokal, M. Somer, P. Notten, H. Hintzen, Sol–gel synthesis and lithium ion conductivity of $\text{Li}_7\text{La}_3\text{Zr}_2\text{O}_{12}$ with garnet-related type structure, *Solid State Ionics* 185 (2011) 42–46.
- [15] S. Hasegawa, N. Imanishi, T. Zhang, J. Xie, A. Hirano, Y. Takeda, O. Yamamoto, Study on lithium/air secondary batteries—stability of nasicon-type lithium ion conducting glass–ceramics with water, *J. Power Sources* 189 (2009) 371–377.
- [16] P. Knauth, Inorganic solid li ion conductors: an overview, *Solid State Ionics* 180 (2009) 911–916.
- [17] N. Imanishi, S. Hasegawa, T. Zhang, A. Hirano, Y. Takeda, O. Yamamoto, Lithium anode for lithium-air secondary batteries, *J. Power Sources* 185 (2008) 1392–1397.
- [18] H. Buschmann, J. Dölle, S. Berends, A. Kuhn, P. Bottke, M. Wilkening, P. Heitjans, A. Senyshyn, H. Ehrenberg, A. Lotnyk, Structure and dynamics of the fast lithium ion conductor “ $\text{Li}_7\text{La}_3\text{Zr}_2\text{O}_{12}$ ”, *Phys. Chem. Chem. Phys.* 13 (2011) 19378–19392.
- [19] X. Liu, J. Fu, C. Zhang, Preparation of nasicon-type nanosized solid electrolyte $\text{Li}_1.4\text{Al}_0.4\text{Ti}_1.6(\text{PO}_4)_3$ by evaporation-induced self-assembly for lithium-ion battery, *Nanoscale Res. Lett.* 11 (2016) 551.
- [20] Y.J. Lim, H.W. Kim, S.S. Lee, H.J. Kim, J.K. Kim, Y.G. Jung, Y. Kim, Ceramic-based composite solid electrolyte for lithium-ion batteries, *ChemPlusChem* 80 (2015) 1100–1103.
- [21] N. Ohta, K. Takada, L. Zhang, R. Ma, M. Osada, T. Sasaki, Enhancement of the high-rate capability of solid-state lithium batteries by nanoscale interfacial modification, *Adv. Mater.* 18 (2006) 2226–2229.
- [22] J.-M. Tarascon, M. Armand, Issues and challenges facing rechargeable lithium batteries, *Materials for Sustainable Energy: A Collection of Peer-Reviewed Research and Review Articles from Nature Publishing Group*, World Scientific, 2011, pp. 171–179.
- [23] B. Scrosati, J. Hassoun, Y.-K. Sun, Lithium-ion batteries. A look into the future, *Energy Environ. Sci.* 4 (2011) 3287–3295.
- [24] D. Lin, W. Liu, Y. Liu, H.R. Lee, P.-C. Hsu, K. Liu, Y. Cui, High ionic conductivity of composite solid polymer electrolyte via in situ synthesis of monodispersed SiO_2 nanospheres in poly (ethylene oxide), *Nano Lett.* 16 (2015) 459–465.
- [25] B. Scrosati, J. Garche, Lithium batteries: status, prospects and future, *J. Power Sources* 195 (2010) 2419–2430.
- [26] A.M. Stephan, K. Nahm, Review on composite polymer electrolytes for lithium batteries, *Polymer* 47 (2006) 5952–5964.
- [27] Y. Liu, J.Y. Lee, L. Hong, Morphology, crystallinity, and electrochemical properties of in situ formed poly (ethylene oxide)/ TiO_2 nanocomposite polymer electrolytes, *J. Appl. Polym. Sci.* 89 (2003) 2815–2822.
- [28] F. Croce, S. Sacchetti, B. Scrosati, Advanced, lithium batteries based on high-performance composite polymer electrolytes, *J. Power Sources* 162 (2006) 685–689.
- [29] Y.-J. Wang, Y. Pan, L. Chen, Ion-conducting polymer electrolyte based on poly (ethylene oxide) complexed with $\text{LiI} \cdot 3\text{aO} \cdot 3\text{TiI} \cdot 7(\text{PO}_4)_3$ salt, *Mater. Chem. Phys.* 92 (2005) 354–360.
- [30] F. Langer, I. Bardenhagen, J. Glenneberg, R. Kun, Microstructure and temperature dependent lithium ion transport of ceramic–polymer composite electrolyte for solid-state lithium ion batteries based on garnet-type $\text{Li}_7\text{La}_3\text{Zr}_2\text{O}_{12}$, *Solid State Ionics* 291 (2016) 8–13.
- [31] D. Lin, Y. Liu, Y. Cui, Reviving the lithium metal anode for high-energy batteries, *Nat. Nanotechnol.* 12 (2017) 194.
- [32] C.-M. Yang, H.-S. Kim, B.-K. Na, K.-S. Kum, B.W. Cho, Gel-type polymer electrolytes with different types of ceramic fillers and lithium salts for lithium-ion polymer batteries, *J. Power Sources* 156 (2006) 574–580.
- [33] C.-Z. Zhao, X.-Q. Zhang, X.-B. Cheng, R. Zhang, R. Xu, P.-Y. Chen, H.-J. Peng, J.-Q. Huang, Q. Zhang, An anion-immobilized composite electrolyte for dendrite-free lithium metal anodes, *Proc. Natl. Acad. Sci. Unit. States Am.* 114 (2017) 11069–11074.
- [34] J. Bae, Y. Li, F. Zhao, X. Zhou, Y. Ding, G. Yu, Designing 3d nanostructured garnet frameworks for enhancing ionic conductivity and flexibility in composite polymer electrolytes for lithium batteries, *Energy Storage Mater.* 15 (2018) 46–52.
- [35] W. Liu, S.W. Lee, D. Lin, F. Shi, S. Wang, A.D. Sendek, Y. Cui, Enhancing ionic conductivity in composite polymer electrolytes with well-aligned ceramic nanowires, *Nat. Energy* 2 (2017) 17035.
- [36] X. Zhang, J. Xie, F. Shi, D. Lin, Y. Liu, W. Liu, A. Pei, Y. Gong, H. Wang, K. Liu, Vertically aligned and continuous nanoscale ceramic–polymer interfaces in composite solid polymer electrolytes for enhanced ionic conductivity, *Nano Lett.* 18 (2018) 3829–3838.
- [37] B. Wicklein, A. Kocjan, G. Salazar-Alvarez, F. Carosio, G. Camino, M. Antonietti, L. Bergström, Thermally insulating and fire-retardant lightweight anisotropic foams based on nanocellulose and graphene oxide, *Nat. Nanotechnol.* 10 (2015) 277.
- [38] H. Kawahara, The structures and functions of ice crystal-controlling proteins from bacteria, *J. Biosci. Bioeng.* 94 (2002) 492–496.
- [39] S. Deville, E. Saiz, R.K. Nalla, A.P. Tomsia, Freezing as a path to build complex composites, *Science* 311 (2006) 515–518.
- [40] M.C. Gutiérrez, M.L. Ferrer, F. del Monte, Ice-templated materials: sophisticated structures exhibiting enhanced functionalities obtained after unidirectional freezing and ice-segregation-induced self-assembly, *Chem. Mater.* 20 (2008) 634–648.
- [41] F. Bouville, E. Maire, S. Deville, Self-assembly of faceted particles triggered by a moving ice front, *Langmuir* 30 (2014) 8656–8663.
- [42] S. Deville, E. Saiz, A.P. Tomsia, Ice-templated porous alumina structures, *Acta Mater.* 55 (2007) 1965–1974.
- [43] D. Clearfield, M. Wei, Investigation of structural collapse in unidirectionally freeze cast collagen scaffolds, *J. Mater. Sci. Mater. Med.* 27 (2016) 15.
- [44] C. Stolze, T. Janoschka, U.S. Schubert, F.A. Müller, S. Flauder, Directional solidification with constant ice front velocity in the ice-templating process, *Adv. Eng. Mater.* 18 (2016) 111–120.
- [45] Y. Zhou, X. Tian, P. Wang, M. Hu, G. Du, Freeze-drying of “pearl milk tea”: a general strategy for controllable synthesis of porous materials, *Sci. Rep.* 6 (2016) 26438.
- [46] J. Zheng, M. Tang, Y.Y. Hu, Lithium ion pathway within $\text{Li}_7\text{La}_3\text{Zr}_2\text{O}_{12}$ -polyethylene oxide composite electrolytes, *Angew. Chem. Int. Ed.* 55 (2016) 12538–12542.
- [47] J. Zheng, Y.-Y. Hu, New insights into the compositional dependence of Li -ion transport in polymer–ceramic composite electrolytes, *ACS Appl. Mater. Interfaces* 10 (2018) 4113–4120.
- [48] L. Chen, Y. Li, S.-P. Li, L.-Z. Fan, C.-W. Nan, J.B. Goodenough, Peo/garnet composite electrolytes for solid-state lithium batteries: from “ceramic-in-polymer” to “polymer-in-ceramic”, *Nanomater. Energy* 46 (2018) 176–184.
- [49] T. Yang, J. Zheng, Q. Cheng, Y.-Y. Hu, C.K. Chan, Composite polymer electrolytes with $\text{Li}_7\text{La}_3\text{Zr}_2\text{O}_{12}$ garnet-type nanowires as ceramic fillers: mechanism of conductivity enhancement and role of doping and morphology, *ACS Appl. Mater. Interfaces* 9 (2017) 21773–21780.



Xue Wang received her Master's Degree in Mechanics Engineering at Harbin Institute of Technology (HIT) in 2016. She is a Ph.D. candidate in Material Science at HIT since 2016, and is currently a two-year joint Ph.D. candidate in Department of Materials Science and Engineering at Columbia University. Her research interests include the design of novel nano-materials, energy materials, solid electrolytes and solid-state batteries.



James Borovilas is an undergraduate studying Applied Physics and Material Science at Columbia University. He is currently slated to receive his B.S. in Applied Physics in 2020. His current research interests focus on investigating the mechanism of lithium dendrite growth on electrolytes by using stimulated Raman scattering microscopy (SRS).



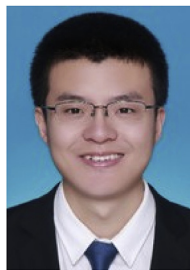
Haowei received his BS (2012) in School of Physics and Technology from Wuhan University, and currently he is a PhD candidate in Department of Applied Physics and Applied Mathematics at Columbia University in the City of New York. His research focuses on solid electrolytes, solid-state batteries, energy materials and nanotechnology.



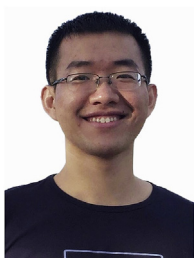
Bingqing Xu received her B.S. in Materials Chemistry from Shandong University in China in 2014. She is a Ph.D. candidate in Materials Science at School of Materials Science and Engineering in Tsinghua University in China since 2014. Now she is a visiting scholar at Department of Materials Science and Engineering in Columbia University. Bingqing's research is mainly on the energy storage materials, lithium sulfur batteries, lithium air batteries, solid lithium batteries, lithium ion capacitors, etc.



Boyu Qie received his bachelor's degree in Chemistry at South University of Science and Technology of China (SUSTC) in 2015, and master's degree in Material Science and Engineering at Columbia University in 2018. His research interests include the design of novel materials and devices for energy storage and conversion, exploration of complex systematic chemistry through molecular self-assembly, and synthesis and application of functional macromolecules and nano-materials.



Changmin Shi received his B.E. in Physical Chemistry within department of Metallurgical Engineering at the University of Science and Technology Beijing in 2017, and M.S. in Materials Science and Engineering at Columbia University in 2019, focusing on energy storage materials.



Qian Cheng received his Ph.D degree major in Materials Science and Engineering at Arizona State University in 2016. He is now a postdoctoral research scientist at Applied Physics & Applied Mathematics in Columbia University. His current research interests focus on investigating the mechanism of lithium dendrite growth on electrolytes by using stimulated Raman scattering microscopy (SRS), improving lithium-sulfur batteries in aspects of both safety and performance, and study of solid electrolyte and their protection.



Tianwei Jin received his B.E. and M.S. degrees at Shanghai University and Columbia University, respectively. His current research interests mainly focus on safety issues of lithium metal batteries and mechanism study on solid electrolytes.



Aijun Li received his Bachelor's degree in Resource Exploration Engineering from Jilin University. He is currently a Ph.D. candidate at School of Earth and Space Sciences, Peking University. His research interests focus on solid-state electrolytes for rechargeable lithium batteries.



Xiangbiao Liao is now a PhD candidate in the Department of Earth and Environmental Engineering under the direction of Prof. Xi Chen at Columbia University. He obtained B.S. degree from University of Science & Technology of China in 2015, majoring in Theoretical and Applied Mechanics. His current research interests lie on engineered morphologies of material structures for energy and environmental applications, including structural designs for flexible and solid state Li-ion battery, catalytic reduction of carbon-dioxide and water collections.



Prof. Yibin Li received his Ph.D from Nanyang Technological University (NTU) in Material Science. He is currently a professor of Center for Composite Material and Structure at Harbin Institute of Technology (HIT). His research interests include nanomaterials, carbon nanotubes fibers, hierarchical composite based on carbon fiber and multiferroic thin films, and ultra-light thermal insulation material.



Martin Dontigny innovates within Hydro-Québec, the company in charge of the generation, transmission and distribution of electricity in the province of Quebec, CA. He currently holds the positions of senior Technologist in cell development and testing at the Center of excellence in transportation electrification and energy storage of Hydro-Quebec [CETEES]. M. Dontigny holds a technical degree from Ahuntsic College, Montreal, and is corresponding author of nearly 20 scientific publications.



Prof. Xiaodong He received his Ph.D from Harbin Institute of Technology (HIT). He is currently a Distinguished Professor of Yangtse River Scholar at HIT. He was awarded the second prize of the National Technology Invention Award in 2012, published 2 monographs and published more than 200 papers in the SCI. His research interests include multi-functional composites, micro-nano mechanics, and thermal insulation composites.



Karim Zaghbi innovates within Hydro-Québec, the company in charge of the generation, transmission and distribution of electricity in the province of Quebec, CA. He holds the positions of General Director at the Center of excellence in transportation electrification and energy storage of Hydro-Quebec [CETEES], CEO of SCE France and CTO of InnovHQ and HQES. His work is paving the way towards the next generation of batteries for electric vehicles. He is a co-inventor in over 550 patents. He is also the author of 393 scientific publications and co-editor of nearly 20 books, including *Lithium Batteries: Science and Technology (2016)*.



Prof. Shanyi Du received his degree from Dept. of Modern Mechanics, University of Science and Technology, China in 1964. He currently works in Center for Composite Material and Structure at Harbin Institute of Technology (HIT) as an honorary director, professor and doctoral supervisor. He is also an executive member of International Committee of Composite Materials. In 1999, he was inducted as a member of the China Engineering Academy. He conducted a systematic study in planning, analyzing and evaluating advanced composite material structure, the mechanics of composites, the micro-mechanics and fracture mechanics, and the intelligent material system and structure.



Yuan Yang is an assistant professor in the Department of Applied Physics and Applied Mathematics, Columbia University. He received his B.S. in physics from Peking University in 2007 and his Ph.D. in materials science and engineering from Stanford University in 2012. Then he worked as a postdoctoral researcher at MIT for 3 years. His research interests include electrochemical energy storage and conversion and thermal management.



Yanke Fu received her Bachelor's Degree in Polymer Materials and Engineering from Beijing University of Chemical Technology in 2016. She received her Master's Degree in Materials Science and Engineering from Columbia University in 2018. Her current research mainly focus on solid state electrolytes for lithium-ion batteries.